Available online at www.sciencedirect.com
SCIENCE DIRECT
Journal of Solid State Chemistry 179 (2006) 1681–1689
JOURNAL OF SOLID STATE CHEMISTRY
www.elsevier.com/locate/jssc

Hydrothermal assembly of (3,6)-connected networks with classical mineral structures constructed from Anderson-type heteropolymolybdate and metal cations

Bo Gao, Shu-Xia Liu*, Lin-Hua Xie, Miao Yu, Chun-Dan Zhang, Chun-Yan Sun, Hai-Yan Cheng

Department of Chemistry, Institute of Polyoxometalate Chemistry, Northeast Normal University, Changchun 130024, P.R. China

Received 11 January 2006; received in revised form 23 February 2006; accepted 25 February 2006
Available online 13 March 2006

Abstract

A series of 3D heteropolymolybdates, $(NH_4)_2\{[M(H_2O)_3]_2[TeMo_6O_{24}]\}\cdot H_2O$ (M = Mn(**1**), Co(**2**), Ni(**3**), Cu(**4**), and Zn(**5**)) and $[Ln(H_2O)_4]_2[TeMo_6O_{24}]\cdot 3H_2O$ (Ln = La(**6**), Ce(**7**), and Nd(**8**)), has been isolated from hydrothermal reactions and characterized by elemental analyses, IR spectra, X-ray crystallography and magnetic properties. Single-crystal X-ray diffraction analysis reveals that compounds **1**–**8** possess unusual (3,6)-connected networks constructed from Anderson-type anions $[TeMo_6O_{24}]^{6-}$ and transion metal or rare-earth metal cations. Compounds **1**–**5** are of highly symmetrical structures with pyrite-like topology in which $[TeMo_6O_{24}]^{6-}$ anions act as 6-connected sites and transition metal cations act as 3-connected sites. Compounds **6**–**8** crystallize in symmetrical space groups lower than that of **1**–**5** exhibiting rutile-like topology with $[TeMo_6O_{24}]^{6-}$ anions acting as 6-connected sites and rare-earth metal cations acting as 3-connected sites. The magnetic properties of **1**–**4** are also presented.

Keywords: Polyoxometalates; Molybdenum; Tellurium; Hydrothermal assembly

1. Introduction

Polyoxometalates (POMs) represent an expanding class of molecular systems, which are of great interest in the fields of catalysis and material science as well as biology, nanotechnology, magnetism, and medicine [1–5]. These fascinating molecular aggregates provide a variety of structural motifs that are potential building blocks for the design and development of extended structures with desirable properties and functions [6,7]. One of the challenging tasks in POM chemistry is to link up discrete polyanion units into one-, two- and even three-dimensional extended solid frameworks in appropriate ways. It is known that transition metal and rare-earth metal ions or their complexes exhibit unique spectroscopic and magnetic properties [8–11], which have wide potential applications. The incorporation of these metal ions into POMs is of interest in material science. Usually, transition metals have less than six coordination numbers and lanthanide prefers coordination numbers of eight and nine. Therefore, lanthanide-containing polyoxoanions [12] and transition-metal-containing anions differ greatly from each other and exhibit unique structures, respectively.

As an important subclass of POMs, Anderson-type heteropolymolybdates exhibiting attractive planar structures can be good candidates for growing porous 3D crystals of nanocomposite compounds [13]. In addition, Anderson-type anions with M=O functionalities can act as multidentate ligands for transition metal or rare-earth metal cations [14,15]. Usually, Anderson-based compounds are mostly synthesized in usual bench conditions and their structures are limited to be mainly one- or two-dimensional structures. However, the hydrothermal synthesis of Anderson-based heteropolyoxometalates remains rarely explored. Recent elaboration has proven that hydrothermal reaction, which causes a reaction shifting from kinetic to thermodynamic domain compared to traditional aqueous

*Corresponding author. Fax: +86 431 5094009.
E-mail address: liusx@nenu.edu.cn (S.-X. Liu).

0022-4596/$ - see front matter © 2006 Elsevier Inc. All rights reserved.
doi:10.1016/j.jssc.2006.02.033

reactions, provides a powerful tool for the synthesis of higher-dimensional oxide frameworks [16].

Herein, we report the hydrothermal synthesis and characterization of a series of new extended 3D compounds: $(NH_4)_2\{[M(H_2O)_3]_2[TeMo_6O_{24}]\}\cdot H_2O$ (M = Mn(**1**), Co(**2**), Ni(**3**), Cu(**4**), and Zn(**5**)) and $[Ln(H_2O)_4]_2[TeMo_6O_{24}]\cdot 3H_2O$ (Ln = La(**6**), Ce(**7**), and Nd(**8**)), which exhibit two types of (3,6)-connected networks. Compounds **1**–**5** are of highly symmetrical 3D frameworks with pyrite-related topology and **6**–**8** are of 3D frameworks with rutile-related topology. In most cases, extended structural compounds with classical mineral structures can be found more easily in metal-organic frameworks (MOFs), such as metal-organic replicas of fluorite [17], pyrite [18], rutile [19], quartz [20], etc. However, compounds **1**–**8** represent the first examples with classical mineral-related topologies constructed from POMs clusters. Furthermore, the magnetic properties of **1**–**4** are also presented.

2. Experimental

2.1. General procedures

All chemicals were analytical reagents, commercially purchased, and used without further purification. Elemental analyses (C, H, N) were performed on a Perkin-Elmer 2400 CHN elemental analyzer. Mn, Co, Ni, Cu, Zn, La, Ce, Nd, Te, and Mo were determined by a PLASMA-SPEC(I) ICP atomic emission spectrometer. IR spectra were recorded in the range 400–4000 cm^{-1} on an Alpha Centaurt FT/IR spectrophotometer using KBr pellets. Magnetic susceptibility data were collected over the temperature range 2–300 K at a magnetic field of 10,000 Oe on a Quantum Design MPMS-5 SQUID magnetometer. TG analysis was performed on a Perkin-Elmer TGA7 instrument in flowing N_2 with a heating rate of 10 °C min^{-1}.

2.2. Synthesis of compounds *1*–*8*

2.2.1. Synthesis of $(NH_4)_2\{[M(H_2O)_3]_2(TeMo_6O_{24})\}\cdot H_2O$ (M = Mn, Co, Ni, Cu, and Zn)

Compound **1** was hydrothermally synthesized under autogenous pressure. A mixture of TeO_2 (0.0828 g), $(NH_4)_6Mo_7O_{24}\cdot 4H_2O$ (0.6231 g), $MnSO_4\cdot 7H_2O$ (0.1502 g), NaOH (0.0451 g), H_2O_2 (30%, 0.5 mL), and H_2O (6 mL) was stirred in air for 1 h after the pH was adjusted to 4.0 with HCl. The resulting suspension was sealed in a 16 mL Teflon-lined stainless-steel autoclave, which was kept at 160 °C for 4 days, then cooled to room temperature at 6 °C h^{-1}. A yellow block crystalline product was recovered by washing with distilled water and filtration. Any impurity was manually removed to give an yield of 73% (based upon Te). Anal. calcd. for $H_{22}Mn_2Mo_6N_2O_{31}Te$ (**1**): H, 1.6; N, 2.1; Mn, 8.1; Te, 9.4; Mo, 42.4. Found: H, 1.7; N, 2.2; Mn, 8.2; Te, 9.3; Mo, 42.5. FT/IR (cm^{-1}) for **1**: 3421(w), 1634(w), 1419(s), 962(s), 913(m), 878(m), 700(s), 656(s).

The preparation of **2** was similar to that of **1**, except that $CoCl_2\cdot 6H_2O$ (0.1352g) was used in place of $MnSO_4\cdot 7H_2O$ (yield: 81% based upon Te). Anal. calcd. for $H_{22}Co_2Mo_6N_2O_{31}Te$ (**2**): H, 1.6; N, 2.0; Co, 8.6; Te, 9.3; Mo, 42.2. Found: H, 1.7; N, 2.1; Co, 8.7; Te, 9.2; Mo, 42.3. FT/IR (cm^{-1}) for **2**: 3426(w), 1639(w), 1417(s), 960(s), 915(m), 878(m), 715(s), 655(s).

The preparation of **3** was similar to that of **1**, except that $NiCl_2\cdot 6H_2O$ (0.1405g) was used in place of $MnSO_4\cdot 7H_2O$ (yield: 66% based upon Te). Anal. calcd. for $H_{22}Ni_2Mo_6N_2O_{31}Te$ (**3**): H, 1.6; N, 2.0; Ni, 8.6; Te, 9.3; Mo, 42.2. Found: H, 1.5; N, 2.2; Ni, 8.7; Te, 9.2; Mo, 42.3. FT/IR (cm^{-1}) for **3**: 3425(w), 1640(w), 1419(s), 961(s), 914(m), 877(m), 714(s), 655(s).

The preparation of **4** was similar to that of **1**, except that $CuCl_2$ (0.0928g) was used in place of $MnSO_4\cdot 7H_2O$ (yield: 57% based upon Te). Anal. calcd. for $H_{22}Cu_2Mo_6N_2O_{31}Te$ (**4**): H, 1.6; N, 2.0; Cu, 9.2; Te, 9.2; Mo, 41.7. Found: H, 3?A3B2 tlsb = -0.02w? > 1.5; N, 2.1; Cu, 9.3; Te, 9.1; Mo, 41.8. FT/IR (cm^{-1}) for **4**: 3434(w), 1634(w), 1412(s), 958(s), 914(m), 878(m), 710(s), 657(s).

The preparation of **5** was similar to that of **1**, except that $Zn(NO_3)_2\cdot 6H_2O$ (0.1645g) was used in place of $MnSO_4\cdot 7H_2O$ (yield: 59% based upon Te). Anal. calcd. for $H_{22}Zn_2Mo_6N_2O_{31}Te$ (**5**): H, 1.6; N, 2.0; Zn, 9.5; Te, 9.3; Mo, 41.9. Found: H, 1.7; N, 2.2; Zn, 9.6; Te, 9.2; Mo, 42.0. FT/IR (cm^{-1}) for **5**: 3433(w), 1638(w), 1421(s), 960(s), 916(m), 876(m), 712(s), 660(s).

2.2.2. Synthesis of $[Ln(H_2O)_4]_2[TeMo_6O_{24}]\cdot 3H_2O$ (Ln = La, Ce, and Nd)

The preparation of **6** was similar to that of **1**, except that $La(NO_3)_3\cdot 6H_2O$ (0.2154g) was used in place of $MnSO_4\cdot 7H_2O$ (yield 83% based upon Te). Anal. calcd. for $H_{22}La_2Mo_6O_{35}Te$ (**6**): H, 1.4; La, 17.8; Te, 8.2; Mo, 36.8. Found: H, 1.3; La, 17.7; Te, 8.1; Mo, 36.9. FT/IR (cm^{-1}) for **6**: 3429(w), 1619(m), 939(s), 890(m), 682(m), 619(s), 533(s), 450(s).

The preparation of **7** was similar to that of **1**, except that $Ce(NO_3)_3\cdot 6H_2O$ (0.2351 g) was used in place of $MnSO_4\cdot 7H_2O$ (yield: 86% based upon Te). Anal. calcd. for $H_{22}Ce_2Mo_6O_{35}Te$ (**7**): H, 1.4; Ce, 17.9; Te, 8.1; Mo, 36.8. Found: H, 1.3; Ce, 17.8; Te, 8.0; Mo, 36.9. FT/IR (cm^{-1}) for **7**: 3431(w), 1621(w), 939(s), 886(m), 686(m), 621(s), 533(s), 450(s).

The preparation of **8** was similar to that of **1**, except that $NdCl_3\cdot 6H_2O$ (0.3011 g) was used in place of $MnSO_4\cdot 7H_2O$ (yield: 66% based upon Te). Anal. calcd. for $H_{22}Nd_2Mo_6O_{35}Te$ (**8**): H, 1.4; Nd, 18.3; Te, 8.1; Mo, 36.6. Found: H, 1.3; Nd, 18.4; Te, 8.0; Mo, 36.7. FT/IR (cm^{-1}) for **8**: 3431(w), 1619(w), 939(s), 885(m), 686(m), 621(s), 533(s), 451(s).

2.3. X-ray crystallography

Crystals of **1**–**8** suitable for single-crystal X-ray diffraction were glued to a thin glass fiber with epoxy resin and mounted to a Rigaku R-AXIS RAPID IP diffractometer

with graphite-monochromated Mo$K\alpha$ ($\lambda = 0.71073$ Å) radiation in the ψ scanning mode at 293 K. The structures were solved by the direct method and refined by full-matrix least squares on F^2 using the SHELXTL-97 software [21]. All of the non-hydrogen atoms were refined anisotropically. The hydrogen atoms were located from the Fourier difference maps. Crystal parameters and details of the data collection and structure refinement for **1–8** are listed in Table 1.

CSD reference nos. for **1–5**: 415245–415249, **6–8**: 415729–415731.

3. Results and discussion

The isolation of compounds **1–8** depends on exploring the conditions of hydrothermal reactions. Usually, it is difficult to optimize the hydrothermal reaction parameters because the reaction system is closed. Many factors, such as starting materials, stoichiometry, pH value, filling volume and temperature, can affect the resulting products. So we carried out a number of parallel experiments to study the reaction parameters to improve the yield and quality of products. During our experiment procedures, we found that the formation of these compounds are very sensitive to the pH value of the reaction system. Another observation we found is that reducing the filling quantity of solid raw materials can lead to high quality of single crystals suitable for X-ray diffraction but at a cost of the yield. We also attempted to synthesize **1–8** via traditional aqueous reactions. However, refluxing the same reaction starting materials under 80 °C for 5 h, we only got some precipitation after a week, which demonstrates that hydrothermal conditions are the requisite factors for preparing compounds **1–8**.

Compounds **1–8** were prepared in the form of highly crystalline materials, and the crystal structures of these compounds were determined by single-crystal X-ray diffraction analysis. The polyanion $[TeMo_6O_{24}]^{6-}$ in each compound is a typical Anderson heteropolymolybdate with D_{3d} symmetry, in which six MoO_6 octahedra form a regular hexagon like a crown and the internal octahedral cavity is filled up by a TeO_6 octahedron. The Te–O bond lengths and O–Te–O bond angles are summarized in Tables 2 and 3, which show only slight distortion of the TeO_6 octahedron. In compounds **1–5**, the MoO_6 octahedron is distorted as expected for a metal atom bound to four types of different oxygen atoms: the oxygen atoms coordinated to two Mo atoms; the oxygen atoms coordinated to a Te atom and two Mo atoms; the oxygen atoms connected with an Mo and a transition metal center; and the terminal oxygen atoms showing the shortest Mo–O bond lengths. In compounds **6–8**, the Mo–O distances can be divided into five groups: the central oxygen atoms connecting with one Te and two Mo atoms; the μ_2-O atoms; the μ_2-O atoms linking to Ln^{III}; the terminal oxygen atoms; the terminal oxygen atoms linking to Ln^{III}. The Mo–O bond lengths and O–Mo–O bond angles, which are typical of those observed for instance in other Anderson-type polyanions, are summarized in Tables 2 and 3.

Compounds **1–5** are of highly symmetrical isomorphous structures, only with some differences among bond lengths and bond angles, therefore we discuss the structure of **1** for example. Compound **1** has a 3D framework constructed from Anderson-type $[TeMo_6O_{24}]^{6-}$ anions with crystallographic $\bar{3}m$ (D_{3d}) symmetry and bridging $\{Mn(H_2O)_3\}$ groups. Here each $[TeMo_6O_{24}]^{6-}$ anion acts as a hexadentate ligand for six Mn (II) atoms, as shown in Fig. 1(a). The six Mn (II) atoms bonding to six terminal oxygen atoms of the Anderson anion are related to each other by $\overline{3}$ symmetry. It is noteworthy that the connectivity behavior between Anderson anions and metal ions is an unusual one when compared with other Anderson-based compounds [14,15], in which Anderson anions usually act as multidentate ligands for less than four metal cations and their connectivity modes are not based on such a symmetric manner. Each Mn (II) cation in **1** is coordinated by three H_2O molecules, three terminal oxygen atoms from three $[TeMo_6O_{24}]^{6-}$ anions, as shown in Fig. 1(b). The coordination geometries of the Mn (II) atoms exhibit distorted octahedra. There is a three-fold axis running through each Mn (II) center, and three H_2O molecules and three $[TeMo_6O_{24}]^{6-}$ anions linked to Mn (II) are related by the three-fold axis. The unusual connection of the alternating $[TeMo_6O_{24}]^{6-}$ anions and $\{Mn(H_2O)_3\}$ groups through corner-shared oxygen atoms results in a 3D (3,6)-connected networks.

Each $[TeMo_6O_{24}]^{6-}$ anion exhibits a planar structure, and six Mn (II) cations bridge the terminal oxygen atoms from above (three Mn (II) ions) and below (three Mn (II) ions) the planar structure. Therefore, $[TeMo_6O_{24}]^{6-}$ anions can be considered as 6-connected sites, and Mn (II) ions may be looked as 3-connected sites if the H_2O molecules coordinated to them are neglected. For perspicuous representation, each 6-connected site is simplified as a distorted octahedron geometry through linking straight the Te center and Mn (II) ions, as shown in Fig. 2(a). The (3,6)-connected net of compound **1** is related to the structure of the pyrite-like of FeS_2; it has the same topology if the S–S bonding in pyrite is ignored. In the structure of pyrite, which has a face-centered cubic symmetry, Fe (II) ions are coordinated by six S^- ions in an octahedron geometry, and S^- ions occupy all the 3-connected sites (Fig. 2c). In compound **1**, $[TeMo_6O_{24}]^{6-}$ anions replace Fe (II) ions and Mn (II) cations replace S^- ions in pyrite. As one can see comparing Figs. 2(b) and (c), the similarities between the structure of compound **1** and genuine pyrite are striking, except for the distortion in the structure of **1**. It is interesting that Anderson-type anions crystallize in such a highly symmetrical space group ($Pa\bar{3}$: identical to pyrite), which has not been observed before. There are two ammonium cations and one H_2O molecule in a molecular unit, filling in the void space of compound **1** with hydrogen bonds between adjacent ammonium cations and H_2O molecules (N1–O4 = 2.838 (6) Å). In the reported literatures, Anderson-type heteropolyanions usually act as

Table 1
Crystal data and structure refinement for **1–8**

Parameter	**1**	**2**	**3**	**4**	**5**	**6**	**7**	**8**
Formula	$H_{22}Mn_2Mo_6N_2O_{31}Te$	$H_{22}Co_2Mo_6N_2O_{31}Te$	$H_{22}Ni_2Mo_6N_2O_{31}Te$	$H_{22}Cu_2Mo_6N_2O_{31}Te$	$H_{22}Zn_2Mo_6N_2O_{31}Te$	$H_{22}La_2Mo_6O_{35}Te$	$H_{22}Ce_2Mo_6O_{35}Te$	$H_{22}Mo_6Nd_2O_{35}Te$
F_w ($g\,mol^{-1}$)	1357.30	1365.28	1364.84	1380.55	1374.13	1563.24	1565.66	1573.90
T (K)	293(2)	293(2)	293(2)	293(2)	293(2)	293(2)	293(2)	293(2)
λ (Å)	0.71073	0.71073	0.71073	0.71073	0.71073	0.71073	0.71073	0.71073
Crystal system	Cubic	Cubic	Cubic	Cubic	Cubic	Monoclinic	Monoclinic	Monoclinic
Space group	$Pa\bar{3}$	$Pa\bar{3}$	$Pa\bar{3}$	$Pa\bar{3}$	$Pa\bar{3}$	$P2_1/n$	$P2_1/n$	$P2_1/n$
a (Å)	14.1477(16)	14.0513(16)	13.9743(16)	14.0087(16)	14.0409(16)	10.130(2)	10.128(2)	10.112(2)
b (Å)						14.239(3)	14.194(3)	14.133(3)
c (Å)						10.385(2)	10.373(2)	10.424(2)
β (deg)						99.66(3)	99.84(3)	99.98(3)
V ($Å^3$)	2831.8(6)	2774.3(5)	2728.9(5)	2749.1(5)	2768.1(5)	1476.7(5)	1469.2(5)	1467.1(5)
Z	4	4	4	4	4	2	2	2
Dc ($g\,cm^{-3}$)	3.184	3.269	3.322	3.336	3.297	3.448	3.539	3.563
μ (mm^{-1})	4.557	4.937	5.183	5.323	5.482	6.376	6.604	7.050
2θ range	$3.22 \leqslant 2\theta \leqslant 27.46$	$3.24 \leqslant 2\theta \leqslant 27.44$	$3.26 \leqslant 2\theta \leqslant 27.47$	$3.25 \leqslant 2\theta \leqslant 27.44$	$2.51 \leqslant 2\theta \leqslant 27.46$	$2.45 \leqslant 2\theta \leqslant 27.48$	$2.46 \leqslant 2\theta \leqslant 27.48$	$3.09 \leqslant 2\theta \leqslant 27.42$
Index range	$-18 \leqslant h \leqslant 18$	$-18 \leqslant h \leqslant 18$	$-18 \leqslant h \leqslant 18$	$-17 \leqslant h \leqslant 18$	$-12 \leqslant h \leqslant 12$	$-13 \leqslant h \leqslant 13$	$-13 \leqslant h \leqslant 13$	$-13 \leqslant h \leqslant 11$
	$-18 \leqslant k \leqslant 16$	$-18 \leqslant k \leqslant 18$	$-18 \leqslant k \leqslant 18$	$-18 \leqslant k \leqslant 18$	$-17 \leqslant k \leqslant 18$	$-17 \leqslant k \leqslant 18$	$-18 \leqslant k \leqslant 18$	$-18 \leqslant k \leqslant 18$
	$-18 \leqslant l \leqslant 18$	$-12 \leqslant l \leqslant 12$	$-18 \leqslant l \leqslant 18$	$-13 \leqslant l \leqslant 13$	$-18 \leqslant l \leqslant 18$	$-13 \leqslant l \leqslant 13$	$-18 \leqslant l \leqslant 16$	$-13 \leqslant l \leqslant 13$
Reflections collected	25,109	24,761	24,055	24,799	2006	6411	6384	13876
Independent reflections	1081	1064	1054	1058	1066	3393	3371	3336
$R_1[I > 2\sigma(I)]$[a]	0.0271	0.0263	0.0413	0.0344	0.0291	0.0606	0.0614	0.0257
$wR_2[I > 2\sigma(I)]$[b]	0.0545	0.0587	0.0809	0.0858	0.0824	0.0883	0.1062	0.0518
R_1 [all data][a]	0.0293	0.0285	0.0531	0.0352	0.0394	0.0802	0.0803	0.0299
wR_2 [all data][b]	0.0551	0.0596	0.0841	0.0863	0.0840	0.0925	0.1113	0.0528

[a] $R_1 = \sum \| F_o | - | F_c \| / \sum | F_o |$.
[b] $wR_2 = \sum [w(F_o^2) - F_c^2] / \sum [w(F_o^2)^2]^{1/2}$.

Table 2
Bond length (Å) and bond angles (deg) with standard deviations in parentheses of compounds **1–5**

	1 (*M*=Mn)	**2** (*M*=Co)	**3** (*M*=Ni)	**4** (*M*=Cu)	**5** (*M*=Zn)
Te–O	1.925(3)	1.930(3)	1.927(4)	1.927(3)	1.927(4)
Mo–O_t	1.706(3)	1.707(3)	1.704(5)	1.705(4)	1.711(5)
Mo–O_{Mo2}	1.927(3)–1.928(3)	1.923(3)–1.931(3)	1.915(5)–1.938(5)	1.916(3)–1.935(3)	1.924(4)–1.933(4)
Mo–O_{TeMo2}	2.262(3)–2.309(3)	2.264(3)–2.314(3)	2.262(5)–2.310(4)	2.270(3)–2.309(3)	2.271(4)–2.312(4)
Mo–O_M	1.724(3)	1.730(3)	1.726(5)	1.730(3)	1.722(4)
M–O_{Mo}	2.163(3)	2.077(3)	2.044(5)	2.082(3)	2.124(4)
M–OH_2	2.157(3)	2.081(3)	2.040(5)	2.049(5)	2.081(4)
O–Te–O_{cis}	85.76–94.24	85.88–94.12	85.89–94.11	85.92–94.08	85.93–94.07
O–Te–O_{trans}	180.0	180.0	180.0	180.0	180.0
O–Mo–O_{cis}	69.94–106.82	70.10–106.47	70.1(2)–106.4(2)	69.99–106.25	69.93–107.0(2)
O–Mo–O_{trans}	152.05–160.05	151.81–159.50	151.5(3)–159.2(2)	151.56–159.75	151.5(2)–160.55
O–M–O	85.58–172.49	87.06–174.99	88.4(2)–176.2(2)	86.87–174.17	86.36–172.78

Table 3
Bond length (Å) and bond angles (deg) with standard deviations in parentheses of compounds **6–8**

	6 (*Ln*=La)	**7** (*Ln*=Ce)	**8** (*Ln*=Nd)
Te–O	1.921(6)–1.935(6)	1.923(6)–1.939(6)	1.925(3)–1.937(3)
Mo–O_t	1.690(7)–1.700(7)	1.684(7)–1.692(7)	1.698(3)
Mo–O_{Mo2}	1.865(7)–1.990(7)	1.858(7)–2.000(7)	1.867(3)–2.002(3)
Mo–O_{TeMo2}	2.198(6)–2.314(6)	2.196(7)–2.310(6)	2.204(3)–2.319(3)
Mo–O_{LnMo2}	1.946(6)–1.997(6)	1.939(6)–2.000(6)	1.951(3)–2.008(3)
Mo–O_{Ln}	1.718(7)–1.731(7)	1.722(7)–1.732(7)	1.721(3)–1.736(3)
Ln–O_{Mo}	2.510(6)–2.570(7)	2.492(6)–2.703(7)	2.464(3)–2.667(3)
Ln–OH_2	2.525(7)–2.564(9)	2.485(8)–2.510(9)	2.459(4)–2.495(4)
O–Te–O_{cis}	84.9(3)–95.1(3)	85.0(3)–95.0(3)	84.7(1)–95.3(1)
O–Te–O_{trans}	180.0	180.0	180.0
O–Mo–O_{trans}	152.7(3)–165.3(3)	152.7(3)–165.5(3)	152.9(1)–165.8(1)
O–Mo–O_{cis}	69.9(2)–107.4(3)	70.3(2)–107.2(3)	70.0(1)–102.1(1)
O–*Ln*–O	59.5(2)–145.1(3)	59.9(2)–143.8(3)	60.3(1)–142.8(1)

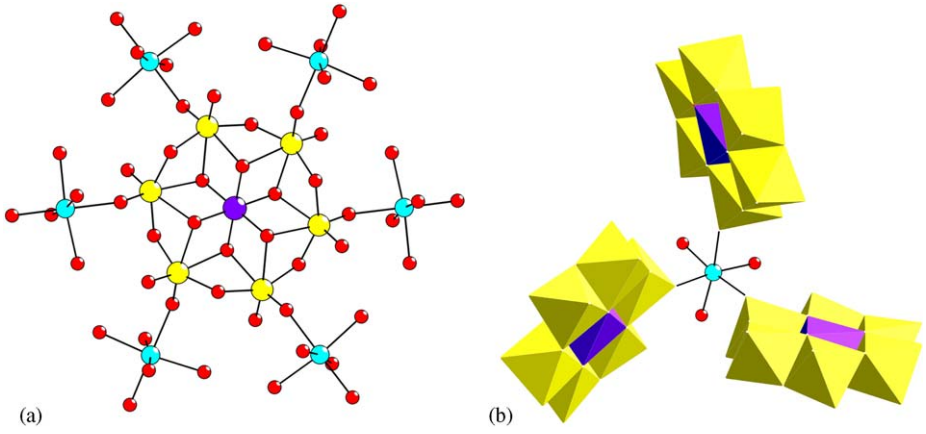

Fig. 1. (a) View of the coordination of an Anderson-type anion $(TeMo_6O_{24})^{6-}$ to six $\{Mn(H_2O)_3\}$ groups; (b) view of the coordination of one $\{Mn(H_2O)_3\}$ group to three $(TeMo_6O_{24})^{6-}$ anions. H_2O molecules coordinated to Mn (II) have been omitted for clarity. Te—purple; Mo—yellow; Mn—blue; O—red; MoO_6 octahedra—yellow; TeO_6 octahedra—purple.

multidentate ligands for rare-earth metal centers. However, first-row transition metals as bridging linkers for Anderson-type anions have been rarely explored. Compounds **1–5** are a series of new examples in which Anderson heteropolyanions are linked through first-row transition metal cations to form a 3D pyrite-like topology.

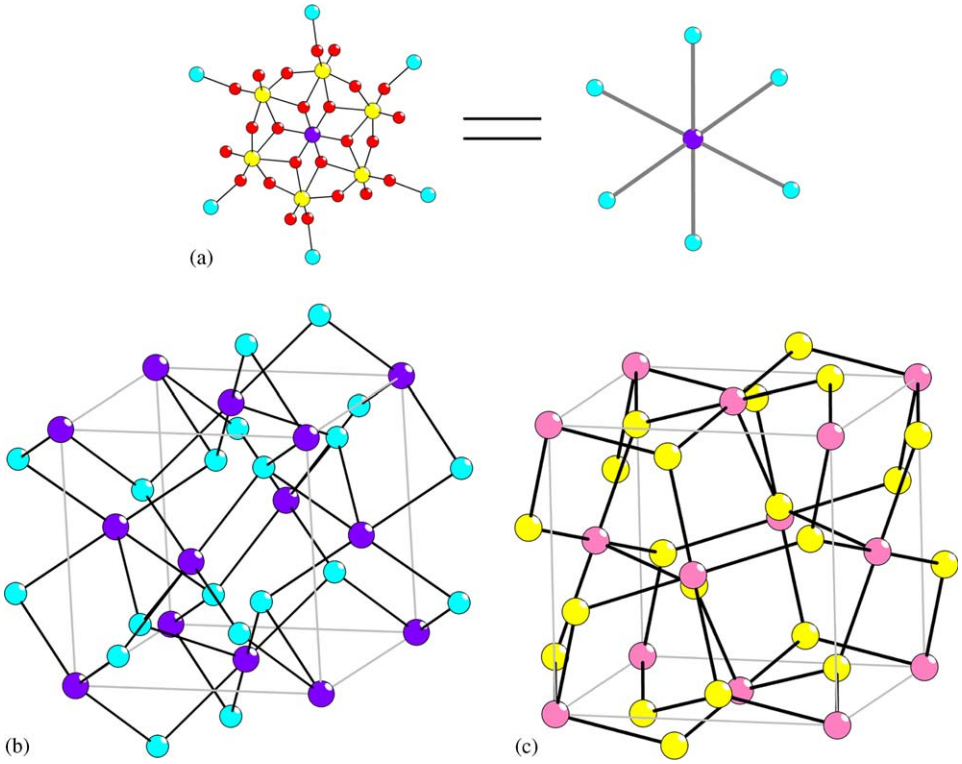

Fig. 2. (a) Simplified view of the 6-connected site as a distorted octahedron geometry in **1**; (b) the simplified structure of pyrite-related networks of **1**; (c) the structure of genuine pyrite. Terminal atoms and H_2O molecules coordinated to Mn (II) have been omitted for clarity in (b) and (c). In (a) and (b), Te—purple; Mo—yellow; Mn—blue; O—red. In (c), Fe—pink; S—yellow.

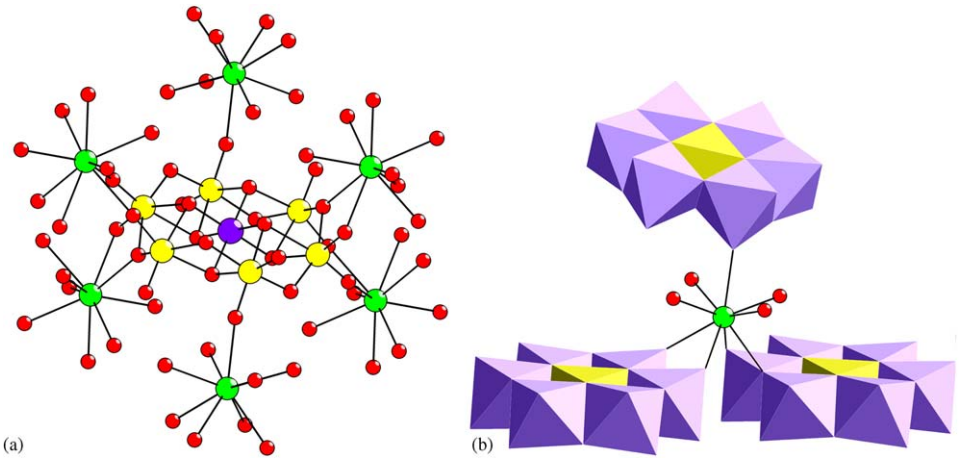

Fig. 3. (a) View of the coordination of an Anderson-type anion $(TeMo_6O_{24})^{6-}$ to six $\{La(H_2O)_4\}$ groups; (b) view of the coordination of one $\{La(H_2O)_4\}$ group to three $(TeMo_6O_{24})^{6-}$ anions. La—green; O—red; MoO_6 octahedra—purple; TeO_6 octahedra—yellow.

Compounds **6–8** crystallize in the same space group $P2_1/n$ with $Z = 4$. Since **7** and **8** are isomorphous with **6**, the structure of **6** is described representatively. Compound **6** has a 3D open framework formed by Anderson-type anions $[TeMo_6O_{24}]^{6-}$ and bridging $\{La(H_2O)_4\}$ groups. It is very interesting that each polyanion $[TeMo_6O_{24}]^{6-}$ acts as a 10-dentate ligand to link up six La^{III} atoms in a center symmetric manner, which has not been observed compared with the Anderson-based compounds reported, as shown in Fig. 3(a). It should be the coordination requirements of rare-earth cations that the Anderson-type anions are able to provide more reactive terminal oxygen atoms even the μ_2-O to connect with lanthanide cations. The six La^{III} atoms exhibit three connecting modes to the Anderson-type anion: the La^{III} atom linking to one terminal oxygen atom; and the La^{III} atom connecting with two terminal oxygen atoms; the La^{III} atom bridging one oxygen atom and one μ_2-O atom. Three La^{III} atoms stand above the planar structure of Anderson polyanion, and the other three below the planar structure, which results in the six

La^{III} atoms relating to each other by central symmetry. Each La^{III} atom, in a distorted tricapped trigonal prism, is coordinated by four H_2O molecules and five oxygen atoms of three Anderson-type anions, in which four are terminal oxygen atoms and one is μ_2-O atom, as shown in Fig. 3(b). Thus, each La^{III} atom links with three Anderson heteropolyanions and each polyanion connects with six $\{La(H_2O)_4\}$ groups, which results in a 3D (3,6)-connected network.

$[TeMo_6O_{24}]^{6-}$ anions can be considered as 6-connected sites, and La^{III} atoms can be looked as 3-connected sites if the coordinated H_2O molecules are ignored. The topology of this network, based on 6- and 3-connected nodes in the ratio 1:2, shows great similarity of the prototypical rutile TiO_2, with $[TeMo_6O_{24}]^{6-}$ anions in the place of Ti and La^{III} atoms in the place of O (see Fig. 4). Since not all the 6-connected nodes or the 3-connected nodes are crystallographically identical to those of rutile's, **6** crystallizes in a lower symmetric space group ($P2_1/n$) than that of rutile ($P4_2/mnm$). In compounds **6**–**8**, the unusual connectivity mode between Anderson-type anion $[TeMo_6O_{24}]^{6-}$ and rare-earth cations results in the higher dimensional frameworks than those by lanthanide polyoxomolybdates containing the heteropolyanion $[TeMo_6O_{24}]^{6-}$ [13], which are limited to be 1D chains.

Bond valence sum calculations [22] indicate that all transition metal centers are in the +2 oxidation state, rare-earth metal centers are in the +3 oxidation state and all Mo and Te sites are in the +6 oxidation state, which reveals that H_2O_2 is possibly responsible for the oxidation of Te(IV) to Te(VI) while stirring under room temperature.

The infrared spectra of compounds **1**–**5** have similar features and also those of **6**–**8** have similar features. In the spectra, the characteristic peaks at 650–1000 cm^{-1} are attributed to the $[TeMo_6O_{24}]^{6-}$ polyoxoanion.

The magnetic susceptibilities of **1**–**4** were investigated from 300 to 2 K, and the temperature dependence of the magnetic susceptibility data are shown in Fig. 5 in the form of the product $\chi_m T$ versus temperature (where χ_m is the magnetic susceptibility per unit of **1**–**4**). In the case of compounds **1**, **3**, and **4**, the $\chi_m T$ products at 300 K are 8.41, 2.34, and 0.91 emu K mol^{-1}, respectively, very nearly equate to the expected values for two uncorrelated M^{2+} centers per formula unit ($\chi_m T$ (**1**) = 8.75 emu K mol^{-1}, $\chi_m T$ (**3**) = 2.00 emu K mol^{-1}, $\chi_m T$ (**4**) = 0.75 emu K mol^{-1}). The $\chi_m T$ values of **1**, **3**, and **4** remain almost constants from 300 to 28 K, 50, and 8 K, respectively, and then decrease on further cooling, reaching a value of 6.59, 1.82, and 0.80 emu K mol^{-1} at 2 K, respectively. For compound **2**, the $\chi_m T$ versus T shows a value of 5.36 emu K mol^{-1} at 300 K (slightly higher than the expected value for two uncorrelated Co^{2+} centers, 3.75 emu K mol^{-1}) and an obvious decreasing trend on cooling to a value of 4.00 emu K mol^{-1} at 10 K, and then drops abruptly below 10 K. The decrease in $\chi_m T$ curves observed in all cases at very low temperatures is mostly due to single-ion zero-field splitting, and perhaps very weak magnetic interactions. From the structures of **1**–**4**, the pathways for magnetic exchange should be through the diamagnetic POM units. Paramagnetic centers are far away from each other, so the magnetic superexchange should be very weak in this case. Curve fits for $1/\chi_m$ versus T plots of **1**, **3**, and **4** are dealt with 2 to 300 K and **2** are from 50 to 300 K with Curie–Weiss law, giving the following results with $C = 8.52$ emu K mol^{-1} and $\theta = 0.83$ K for **1**, $C = 6.10$ emu K mol^{-1} and $\theta = -12.45$ K for **2**, $C = 2.35$ emu K mol^{-1} and $\theta = 1.06$ K for **3**, and $C = 0.91$ emu K mol^{-1} and $\theta = 0.81$ K for **4**.

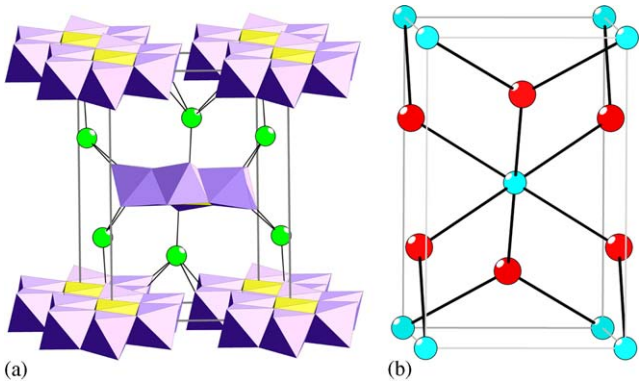

Fig. 4. (a) The structure of rutile-related networks of **1**; (b) the structure of genuine rutile-TiO_2. Terminal atoms and H_2O molecules coordinated to La(III) have been omitted for clarity in (a) and (b). In (a), TeO_6 octahedra—yellow; MoO_6 octahedra—purple; La—green. In (b), O—red; Ti—blue.

Thermogravimetric measurements of compounds **1** and **6** are investigated as representatives. For compound **1**, guest and coordinated water molecules as well as ammonium cations are released between 100 and 400 °C with a weight loss of 12.85% (calc. 11.93%). The weight remains the same between 400 and 690 °C, indicating that the framework of compound **1** is stable in this temperature range. And then the framework starts to collapse from 690 °C. For compound **6**, between 40 and 470 °C there are three steps of weight loss in total 12.76% (calc. 12.66%) corresponding to the release of guest and coordinated water molecules. The framework is stable up to 760 °C, and then starts to collapse. From the thermogravimetric measurements of compounds **1** and **6**, we can reach a conclusion that the frameworks of compounds **1**–**8** can still be maintained in a certain wide temperature range after losing their guest molecules, even coordinated water molecules.

4. Conclusions

In summary, a series of unprecedented 3D extended structure materials constructed from Anderson-type heteropolyanions and metal ions has been presented. A particular novel feature of these compounds is their attractive mineral topologies, which have been rarely found in POMs. The successful isolation of **1**–**8** suggests that hydrothermal synthesis is an effective method to

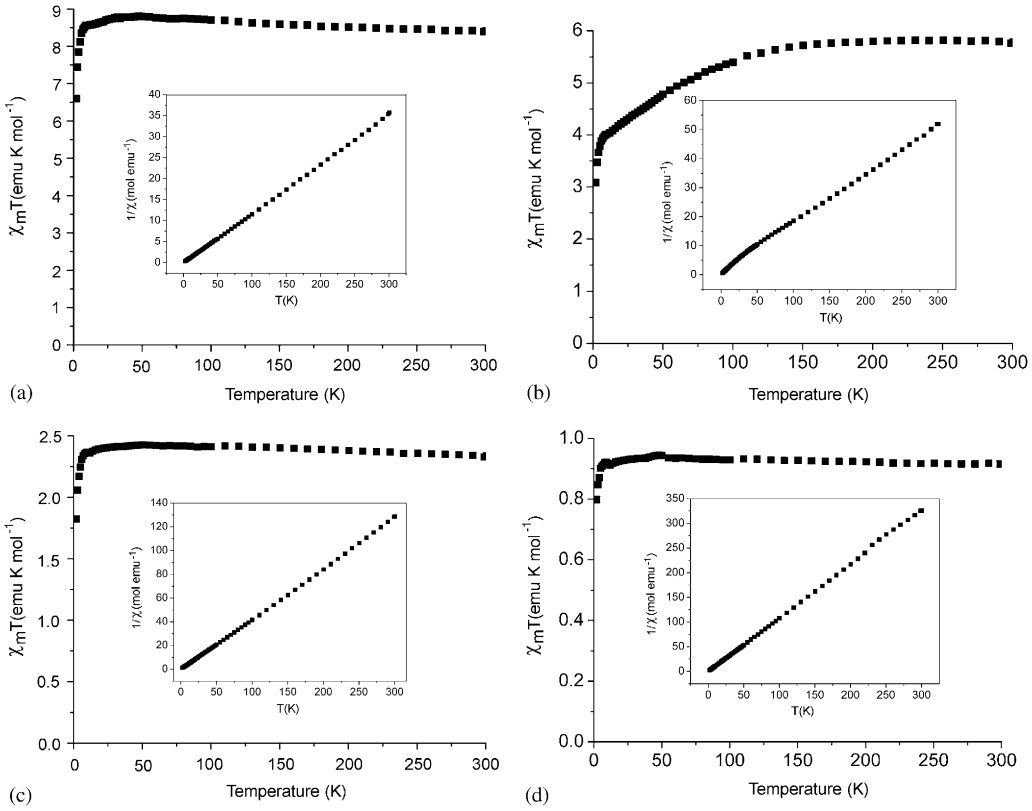

Fig. 5. Temperature dependence of magnetic susceptibility given by measurements of $\chi_m T$ at 1 T over a temperature range 2–300 K. (a) compound **1**; (b) compound **2**; (c) compound **3**; (d) compound **4**. The inset figures show the inverse susceptibility with a linear regression based on the Curie–Weiss law.

construct some higher-dimensional frameworks for Anderson-based new compounds or possibly other POMs-based compounds are compared with traditional aqueous reactions.

Acknowledgment

This work was financially supported by the National Natural Science Foundation of China (No. 20571014) and the Scientific Research Foundation for Returned Overseas Chinese Scholars, the Ministry of Education.

References

[1] M.T. Pope, Heteropoly and Isopoly Oxometalates, Springer, Berlin, 1983.
[2] M.T. Pope, A. Müller, Polyoxometalates: From Platonic Solids to Anti-Retroviral Activity, Kluwer Academic Publishers, Dordrecht, 1994.
[3] C.L. Hill, C.M.P. McCartha, Coord. Chem. Rev. 143 (1995) 407.
[4] C.L. Hill, et al., Chem. Rev. 98 (1998) 1.
[5] M.T. Pope, A. Müller, Polyoxometalate Chemistry: From Topology via Self-Assembly to Applications, Kluwer Academic Publishers, Dordrecht, 2001.
[6] J.R. Galán-Mascarós, C. Giménez-Saiz, S. Triki, C. Gómez-García, E. Coronado, L. Ouahab, Angew. Chem. Int. Ed. 34 (1995) 1460;
P.J. Hagrman, D. Hagrman, J. Zubieta, Angew. Chem. Int. Ed. 38 (1999) 2638.
[7] M.I. Khan, E. Yohannes, D. Powell, Chem. Commun. 12 (1999) 23;
M.I. Khan, E. Yohannes, R.J. Doedens, Angew. Chem. Int. Ed. 38 (1999) 1292;
M.I. Khan, J. Solid State Chem. 152 (2000) 105;
M.I. Khan, E. Yohannes, R.J. Doedens, Inorg. Chem. 42 (2003) 3125.
[8] R.C. Howell, F.G. Perez, S. Jain, W.D. Horrocks Jr., A.L. Rheingold, L.C. Francesconi, Angew. Chem. Int. Ed. 40 (2001) 4031.
[9] M. Elhabiri, R. Scopelliti, J.-C.G. Bünzli, C. Piguet, J. Am. Chem. Soc. 121 (1999) 10747.
[10] J. Lü, E. Shen, M. Yuan, Y. Li, E. Wang, C. Hu, L. Xu, J. Peng, Inorg. Chem. 42 (2003) 6956.
[11] M.I. Khan, E. Yohannes, R.C. Nome, S. Ayesh, V.O. Golub, C.J. O'Connor, R.J. Doedens, Chem. Mater. 16 (2004) 5273.
[12] C.D. Wu, C.Z. Lu, H.H. Zhuang, J.S. Huang, J. Am. Chem. Soc. 124 (2002) 3836;
M. Sadakane, M.H. Dickman, M.T. Pope, Angew. Chem. Int. Ed. 39 (2000) 2914;
P. Mialane, L. Lisnard, A. Mallard, J. Marrot, E. Antic-Fidancev, P. Aschehoug, D. Vivien, F. Se'cheresse, Inorg. Chem. 42 (2003) 2102.
[13] J.-H. Son, H. Choi, Y.-U. Kwon, J. Am. Chem. Soc. 122 (2000) 7432.
[14] H. An, D. Xiao, E. Wang, Y. Li, L. Xu, New J. Chem. 29 (2005) 667;
H. An, E. Wang, D. Xiao, Y. Li, L. Xu, Inorg. Chem. Commun. 8 (2005) 267;
H. An, E. Wang, D. Xiao, Y. Li, L. Xu, Inorg. Chem. Commun. 8 (2005) 267;
D. Drewes, B. Krebs, Z. Anorg. Allg. Chem. 631 (2005) 2591;
D. Drewes, E.M. Limanski, B. Krebs, Eur. J. Inorg. Chem. (2004) 4849;
D. Drewes, E.M. Limanski, B. Krebs, Dalton Trans. (2004) 2087;
V. Shivaish, P.V. Narasimha Reddy, L. Cronin, S.K. Das, Dalton Trans. (2002) 3781.

[15] H. An, Y. Guo, Y. Li, E. Wang, J. Lü, L. Xu, C. Hu, Inorg. Chem. Commun. 7 (2004) 521;
V. Shivaish, M. Nagaraju, S.K. Das, Inorg. Chem. 42 (2003) 6604.
[16] J.Y. Lu, M.L. Lawandy, J. Li, T. Yuen, C.L. Lin, Inorg. Chem. 38 (1999) 2695;
Gopalakrishnan, J. Chem. Mater. 7 (1995) 1265.
[17] H. Chun, D. Kim, D.N. Dybtsev, K. Kim, Angew. Chem. Int. Ed. 43 (2004) 971.
[18] H.K. Chae, J. Kim, O.D. Friedrichs, M. O'Keeffe, O.M. Yaghi, Angew. Chem. Int. Ed. 42 (2003) 3907.
[19] L. Xie, S. Liu, B. Gao, C. Zhang, C. Sun, D. Li, Z. Su, Chem. Commun. 18 (2005) 2402;
C. Qin, X. Wang, L. Carlucci, M. Tong, E. Wang, C. Hu, L. Xu, Chem. Commun. 17 (2004) 1876;
S.R. Batten, B.F. Hoskins, R. Robson, J. Chem. Soc. Chem. Commun. 4 (1991) 445;
S.R. Batten, B.F. Hoskins, B. Moubaraki, K.S. Murray, R. Robson, J. Chem. Soc. Dalton Trans. (1999) 2977.
[20] B.F. Hoskins, R. Robson, N.V.Y. Scarlett, Angew. Chem. Int. Ed. 34 (1995) 1203;
J. Sun, L. Weng, Y. Zhou, J. Chen, Z. Chen, Z. Liu, D. Zhao, Angew. Chem. Int. Ed. 41 (2002) 4471.
[21] G.M. Sheldrick, SHELXS 97, Program for Crystal Structure Solution, University of Göttingen, Göttingen, Germany, 1997;
G.M. Sheldrick, SHELXS 97, Program for Crystal Structure Refinement, University of Göttingen, Göttingen, Germany, 1997.
[22] D. Brown, D. Altermatt, Acta Crystallogr. B 41 (1985) 244.